Characteristics of Small Molecule Compounds Produced from the Co-pyrolysis of Cotton Stalk and Coal

Chuyang Tang, Lei Yang, Xianchun Li,* and Jinling Song

Pyrolysis experiments of cotton stalk (CS) and Shenmu coal (SM) were conducted in a tubular furnace. The pyrolysis temperature was 600 °C at 5 °C/min and sustained for 15 min. The water-soluble small molecule compounds (WSMC) were derived from the liquid products obtained during pyrolysis with the methods of toluene entrainment and ultrasonic extraction. The compositions of WSMC were further characterized by gas chromatography–mass spectrometry (GC-MS). The components of the syngas were analyzed by gas chromatography (GC). The results showed that the phenol yield was promoted by the interaction of CS and SM during co-pyrolysis. Moreover, the co-pyrolysis interaction blocked the radical reaction pathway that produces amides and accelerated the formation of pyridines. Because the ester yield increased, the esterification was clearly enhanced and the yield of carboxylic acids in WSMC was reduced during co-pyrolysis. In addition, the inhibition of furan generation resulted in an increased yield of C2–C4 hydrocarbons in the co-pyrolysis syngas. The maximal yields of C2–C4 hydrocarbons all occurred at a 20/100 ratio of CS/SM. Lastly, the formation mechanisms of small molecule compounds were proposed.

Keywords: Co-pyrolysis; Cotton stalk; Coal; Small molecule compound; Syngas

Contact information: School of Civil Engineering, University of Science and Technology Liaoning, 185#, Qianshan Road, Liaoning Province 114051, PR China;
** Corresponding author: askd1972@163.com*

INTRODUCTION

China has an abundance of biomass and coal, but direct combustion of crop stalks and coal has caused environmental concerns in recent decades (Malen and Marcus 2017; Liang *et al*. 2020). Co-pyrolysis has been considered to be a promising technical approach to produce drop-in hydrocarbon fuels and added-value chemicals from biomass and coal (Hassan *et al*. 2016; Wei *et al.* 2017). Nevertheless, multiple challenges remain to fully understand the effects of co-pyrolysis processes on the pyrolytic products. Most tars produced from co-pyrolysis of biomass and coal have low energy density and stability (Zhu *et al*. 2020). Extensive technical efforts have been performed to understand the effects, but the improvement approaches have provided few answers. Recent studies revealed that the product distribution of co-pyrolysis was determined by the complicated physical-chemical reactions between biomass and coal, *i.e*., interactions (Krerkkaiwan *et al.* 2013; Wu *et al*. 2015; Abdelsayed *et al.* 2019). Because the oxygen/carbon ratio and thermo-chemical reactivity of biomass were obviously higher than those of coal, the co-pyrolysis interactions affected the categories and yields of the compounds in tar (Abnisa and Daud 2014; Yang *et al.* 2014).

Co-pyrolysis tar is a complex mixture of hundreds of chemicals, including aliphatic hydrocarbons, aromatics, carboxylic acids, furans, and esters (Zhang *et al*. 2007). The

carboxylic acid is highly corrosive and reduces the combustion performance of co-pyrolysis tar. Compared with petroleum, co-pyrolysis tar has more compounds with unsaturated bonds and oxygen-containing functional groups (Li *et al*. 2020). The co-pyrolysis tar is reactive and ages quickly. Therefore, this kind of tar is difficult to upgrade at an acceptable cost. The aliphatic hydrocarbons and aromatics are also rich in petroleum, as is well known. The water-soluble small molecule compounds (WSMC) should be the dominant factor leading to the instability of co-pyrolysis tar. Many studies have reported that WSMC was detected in the co-pyrolysis tar of biomass and coal (Weiland *et al.* 2012; Lievens *et al.* 2013). However, there has been little research on the characteristics of the WSMC yields and categories, because the WSMC is difficult to separate from the pyrolytic liquid products.

The authors of the current study previously published a reliable method to extract WSMC from the pyrolytic liquid products (Tang *et al.* 2015). The work demonstrated the possibility of performing a quantitative study of WSMC formation during co-pyrolysis of biomass and coal. In general, co-pyrolysis can be understood as free radical reactions (Li *et al.* 2013b). The blends of biomass and coal usually start with the thermal cleavage of covalent bonds to generate volatile radical fragments at temperatures between 285 and 475 °C (Lu *et al.* 2013). Most small molecule compounds (including WSMC and syngas) are generated within this temperature range. Liu *et al.* (2016) indicated that the generation and reaction of free radicals determined the product distribution during low temperature pyrolysis. He *et al.* (2014) revealed that the small molecule compounds still had significant effects on the stability of tars even after pyrolytic processes. The formation of small molecule compounds explains the poor quality and instability of pyrolytic tars (Meng *et al.* 2015).

The authors recently focused on improving the quality and yields of tar during the co-pyrolysis of biomass and coal. Compared with cotton stalk (CS) pyrolysis and Shenmu coal (SM) pyrolysis, it was found that the formation of strong-polar compounds was obviously restrained during the co-pyrolysis of CS and SM. In this study, the WSMC were derived from liquid products by toluene entrainment and microwave-assisted extraction. The compounds in WSMS were then analyzed by gas chromatography-mass spectrometry (GC-MS), and the syngas components were detected by GC. Possible formation mechanisms of small molecule compounds in co-pyrolysis are proposed based on free radical reactions.

EXPERIMENTAL

Raw Materials and Process of Pyrolysis

The materials used in this study were Shenmu bituminous coal (assigned as SM; from Shanxi province, China), cotton stalk (assigned as CS; Shandong province, China), and biomass-coal blends at ratios of 5/100, 10/100, 20/100, 30/100, and 50/100. The air-dried materials were milled and sieved to obtain fractions of particles sized less than 180 μm in diameter for both SM and CS. Next, the samples were dried at 105 °C for 2 h and then stored in a desiccator. Ultimate analyses were determined using a Macro Cube (Elementar; Berlin, Germany). The properties of samples are listed in Table 1. According to the results of proximate analyses, the CS volatile matter was much higher than that of SM, whereas the fixed carbon showed inverse results. The analysis suggested that CS had a higher thermal reactivity than SM. The H content of CS was higher than that of SM. The

ultimate analysis also showed that the O/C ratio of CS (92.91) was markedly higher than that of SM (10.54) due to more oxygen-containing functional groups in CS. The pyrolysis experiments were conducted in a tubular furnace (from room temperature to 600 °C at 5 °C/min, then sustained for 15 min), as was this research group's previous work (Tang *et al*. 2015). The syngas was collected by gasbag. The volatiles released from the sample were cooled in a condenser in series to collect the condensable components. The liquid products were recovered by washing the sample with methylbenzene (AR grade) and were collected in a round bottom flask. The liquid (including tar, WSMC, and water) yield of pyrolysis was determined by the varied weight of the condenser, reactor, and pipeline before and after washing. The char yield was determined by weighing the amount of the solid residue in the reactor. The pyrolytic water and WSMC were then separated by the toluene entrainment method according to ASTM D4006-16e1 (2016). Methylene chloride (AR grade) was chosen as the extractant. The WSMC compounds were then extracted from pyrolytic water by ultrasonic-assisted extraction at 0 °C. The pyrolytic water yield was determined by the weight of the removed WSMC water and the proximate analyses of SM and CS. The tar yield was the difference in value of the yield of liquid products, namely, the WSMC yield and the water yield.

Table 1. Proximate and Ultimate Analyses of the Samples (Tang *et al.* 2015)

Sample	SM	CS
Proximate Analysis (wt%)		
Moisture (ad[a])	3.78	2.31
Ash (d[d])	8.63	4.13
Volatile matter (daf[a])	37.97	78.88
Fixed carbon (daf)	62.03	21.12
Ultimate Analysis (wt%, daf)		
Carbon (C)	84.24	48.11
Hydrogen (H)	5.49	6.02
Nitrogen (N)	1.08	0.98
Sulfur (S)	0.32	0.19
Oxygen (O) (diff[b])	8.88	44.70
[a] ad, air-dried benchmark; [d]d, dry benchmark; daf, dry and ash-free benchmark; [b] calculated by difference		

Methods

GC-MS analyses of WSMC

The compounds dissolved in methylene chloride were then analyzed by GC-MS (Agilent 5975C; Agilent Technologies, Santa Clara, CA, USA). High-purity helium was chosen as the carrier gas. The injection and ion-resource temperatures were set at 250 °C. The mass spectrometer was used in the electron ionization mode at 70 eV in the range of 33 to 500 *m*/*z*. The content of each compound in the WSMC was calculated as the relative peak area against the total peak area (excluding that of the solvent) in the total ion chromatogram of GC-MS. The yield of each compound was defined as the mass percentages of the product against the mass of the test sample (dry and ash free basis).

GC analyses of syngas

The syngas components were detected by a GC 126 (INESA Instrument Co., Shanghai, China), equipped with a flame ionization detector and a thermal conductivity

detector. The GC 126 analyzed the major components (H_2, CH_4, CO, CO_2, and C2−C4 hydrocarbons) of syngas.

RESULTS AND DISCUSSION

Pyrolytic Characteristics of SM and CS

The distribution of co-pyrolysis products for SM and CS in the tubular furnace are illustrated in Fig. 1a. All yields are represented in mass percentage on dry and ash free benchmark. The CS pyrolysis results included the maximal syngas yield, tar yield, water yield, and WSMC yield, which were 24.49 wt% (daf), 14.37 wt% (daf), 20.70 wt% (daf), and 11.23 wt% (daf), respectively.

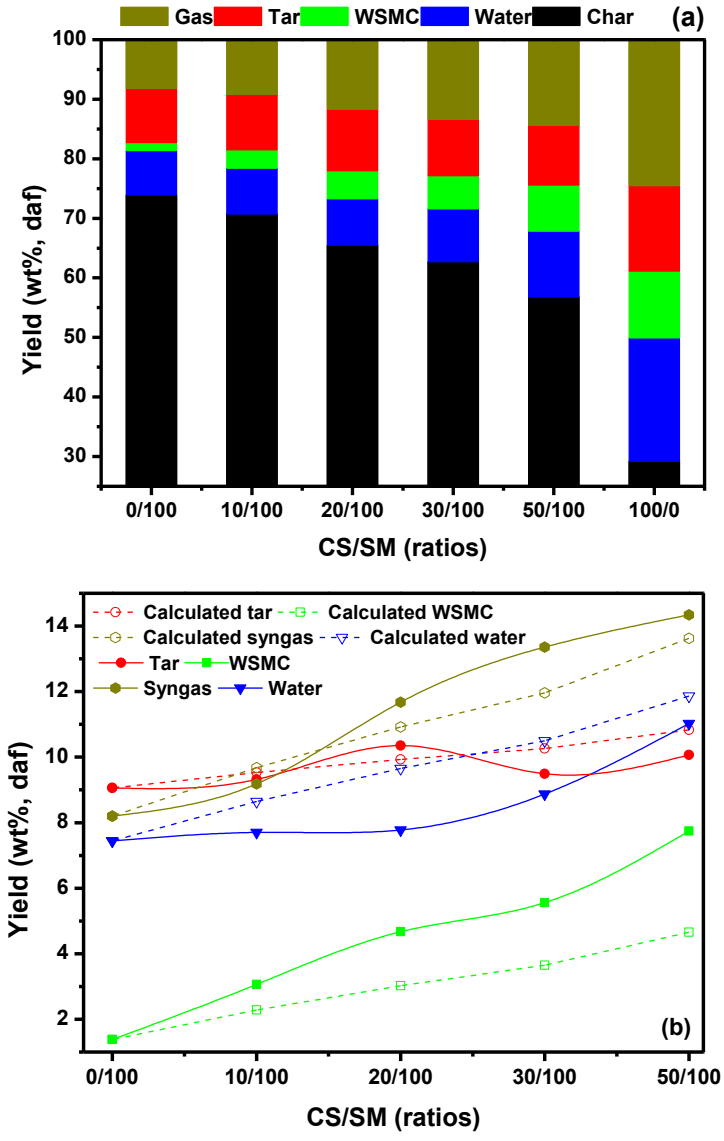

Fig. 1. Co-pyrolysis of CS and SM at different blending ratios: a) difference of product yields; b) difference of product yields with the calculated values

As shown, the CS pyrolysis produced more syngas, tar, and WSMC than the SM pyrolysis did. The water yield of CS pyrolysis was much higher than that of SM pyrolysis due to the higher oxygen content of CS. The char yield of CS pyrolysis was lower than that of SM pyrolysis, corresponding to the proximate analyses of CS and SM. The char yield decreased with the CS ratio of blend, increasing with the co-pyrolysis of CS and SM, but the syngas yield, tar yield, water yield, and WSMC yield were the opposite.

The product yield from the co-pyrolysis of CS/SM was compared with its calculated value in Fig. 1b. The results indicated that there was clearly an interactive effect between CS and SM during co-pyrolysis. The curve of WSMC yields was always above the curve of the calculated WSMC yields. It was clear that CS as an additive improved the co-pyrolysis of CS and SM to produce more WSMC than SM pyrolysis alone. The syngas yields were higher than the calculated values when the content ratio of the CS/SM blend was greater than 15/100. The results highlighted that the cleavage of the CS structure generated more volatile fragments than SM pyrolysis when forming gas during co-pyrolysis. The authors' previous work found that the co-pyrolysis tar used in this study was mainly composed of aliphatic hydrocarbons, benzenes, and polyaromatic hydrocarbons (PAHs) (Tang and Zhang 2016). The tar yields were first increased and then decreased with the increase of CS content, in comparison with the calculated values. The tar yields were greater than the calculated values, within the ratio rang of the CS addition between 15/100 and 25/100 of CS/SM blends. Moreover, the maximal tar yield (10.35 wt%, daf) occurred at the CS/SM ratio of 20/100, which was clearly higher than its calculated value. Based on the CS/SM blend ratio of co-pyrolytic experiments, the water yields were always lower than the relevant calculated values. The lowest yield of water yield (7.78 wt%, daf) was obtained at the ratio of 20/100 and was 18.86% lower than its calculated value (9.65 wt%, daf). The interaction clearly affected the distribution of co-pyrolysis products. Concerning free radicals, more tar was produced at a proper blending ratio during co-pyrolysis because the free radicals released from CS stabilized the macromolecule free radicals generated from SM pyrolysis, forming aliphatic hydrocarbons and aromatics (Sonobe *et al.* 2008). Many alkyl radicals were generated from the cleavage of side chains and bridged bonds in coal's aromatic structure during SM pyrolysis. Correspondingly, the CS pyrolysis produced more oxygen-containing radicals than SM pyrolysis in accordance with the mechanism of biomass pyrolysis (Gu *et al.* 2013). Therefore, the free radicals from CS pyrolysis also promoted the yields of syngas and WSMC when the CS ratio increased in the CS/SM blend during co-pyrolysis. Meanwhile, the radical reaction of pyrolytic water formation was suppressed. Because the generation of free radicals was affected by the compositions and chemical structures of CS and SM, further experiments were performed to investigate the mechanism, described as follows.

WSMC Characterization Derived from Pyrolysis

The categories and yields of WSMC were calculated by the results of GC-MS analyses and are presented in Fig. 2a. It was apparent that the WSMC of CS pyrolysis was quite different from that of SM pyrolysis. Compared with SM pyrolysis, CS pyrolysis produced more diverse kinds of WSMC, such as esters, carboxylic acids, furans, alcohols, and amides. The ketone yield of CS pyrolysis was 2.36 wt% (daf), far greater than that of SM pyrolysis (0.12 wt%, daf). Furthermore, the yields of phenols and aldehydes derived from CS pyrolysis were much higher than those from SM pyrolysis. As can be seen in Fig. 2a, amides were not detected in the WSMC generated from the co-pyrolysis of CS and SM. Moreover, the yield of pyridines from co-pyrolysis (0.28 wt%, daf) was clearly higher than

that from CS pyrolysis and SM pyrolysis. The chemical property of pyridine is similar to nitrobenzene and its aromaticity is lower than benzene. The results demonstrated that the co-pyrolysis interaction remarkably influenced the occurrence and distribution of nitrogen in WSMC.

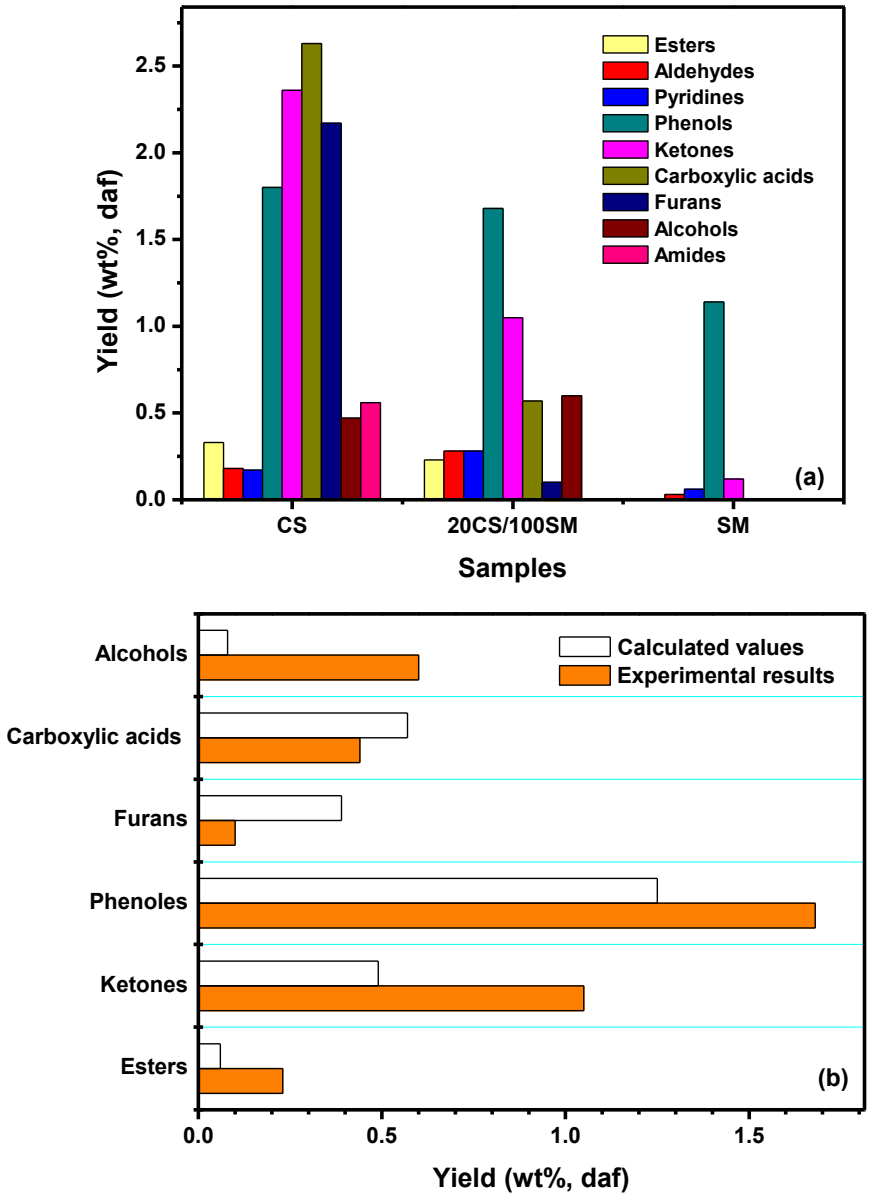

Fig. 2. Characterization of WSMC derived from the pyrolysis of CS and SM (a: categories and yields of WSMC; b: difference of WSMC yields with the calculated values at a 20/100 ratio of CS/SM)

In general, pyridines were generated from the condensation reaction between the nitrogenous radicals and the alkyl radicals with two unpaired electrons during the co-pyrolysis of CS and SM. If the alkyl radicals were scarce, the radical reaction tended to produce amides. The SM produced many alkyl radicals through the cleavage of the alkyl side chain and bridged bond during co-pyrolysis. For the analysis, it was clear that the co-

pyrolysis interaction blocked the pathway of amide generation and promoted pyridine production.

The yield of carboxylic acids from co-pyrolysis (0.44 wt%, daf) was lower than its calculated value (shown in Fig. 2b). The yield of alcohols from co-pyrolysis (0.60 wt%, daf) was far more than the calculated value (0.08 wt%, daf). The yield of esters was 0.23 wt% (daf) and, consequently, greater than the calculated value (0.06 wt%, daf). The results demonstrated that esterification produced more esters and decreased the yield of carboxylic acids due to the increased generation of alcohols during co-pyrolysis. Moreover, the co-pyrolysis of CS and SM improved the formation of phenols in WSMC, which was 1.68 wt% (daf) and higher than its calculated value (1.25 wt%, daf). The results suggested that the free radicals from CS pyrolysis improved the stabilization of phenols on co-pyrolysis. In summary, the interaction of CS/SM co-pyrolysis selectively accelerated the formation of phenols, ketones, esters, alcohols, and furans in WSMC.

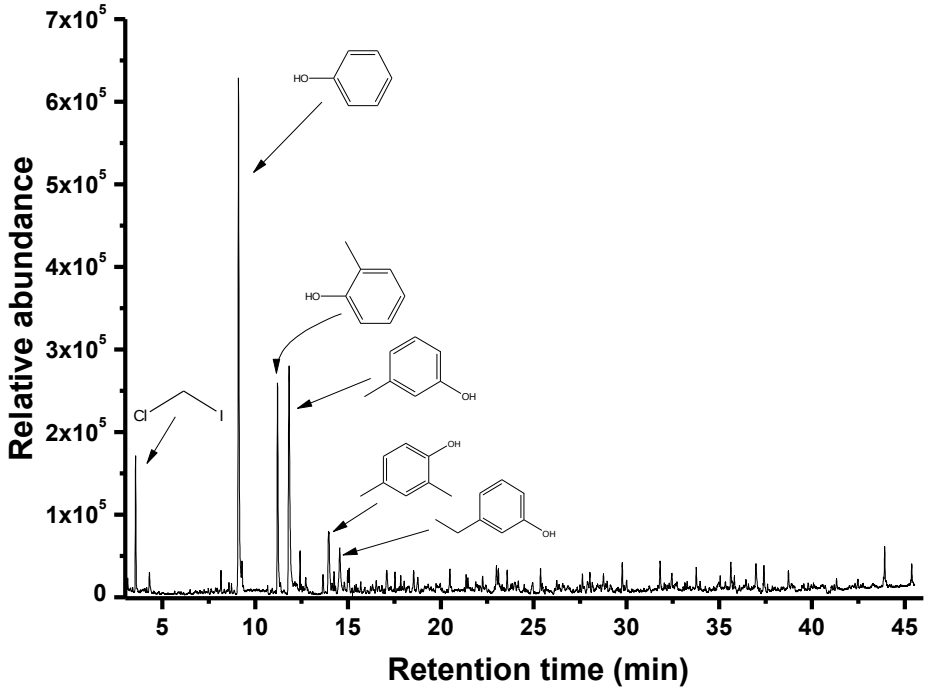

Fig. 3. Chromatogram of GC-MS results for WSMC from SM co-pyrolysis

As shown in Fig. 3, the main compounds in the WSMC of SM pyrolysis were phenol and its derivatives. Figure 4 shows the GC-MS analysis of WSMC from CS pyrolysis. It differed from SM pyrolysis in that CS pyrolysis produced more diverse oxygenated chemicals. Furthermore, most phenols from CS pyrolysis had the side chain of methoxyl or carboxyl. Based on the chemical construction of CS, the results showed that most of the phenols were generated from the thermal decomposition of lignin during CS pyrolysis. The results in Fig. 2b show that the yield of phenols in co-pyrolysis was greater than its calculated value. The most generated phenols were aromatic radicals during co-pyrolysis. Phenol radicals combined with micromolecular radicals (such as alkyl radical, ethyl radical, hydroxyl radical, and so on), which then stabilized into phenols. Compared with individual SM pyrolysis, it was evident that more phenol radicals separated from the SM aromatic nucleus and reacted with the alkyl and hydroxyl radicals from SM

decomposition, further generating more phenols during the co-pyrolysis of CS and SM (at a 20/100 ratio). In addition, the GC-MS results showed that the WSMC from CS pyrolysis were rich in carboxylic acids, which consisted mostly of acetic acid (0.77 wt%, daf), propionic acid (0.11 wt%, daf), butyric acids (0.06 wt%, daf), and aliphatic acids (0.05 wt%, daf). The acetic acid yield accounted for 76.46 wt% of the carboxylic acids. This type of carboxylic acid was not detected in the WSMC from SM pyrolysis (results in Fig. 4). Dong *et al.* (2012) reported that carboxylic acids were mainly derived from cellulose decomposition during poplar wood pyrolysis. The study confirmed that carboxylic acids were mainly produced from CS during co-pyrolysis. Figure 5 shows the GC-MS analysis of WSMC from the co-pyrolysis of CS and SM at a 20/100 ratio. Acetic acid was not detected in the WSMC of co-pyrolysis. Acetic acid most easily reacted with alcohols, compared with other carboxylic acids detected in the WSMC of CS pyrolysis. Figures 2 and 5 further demonstrate that esterification improved the ester yield from the co-pyrolysis of CS and SM.

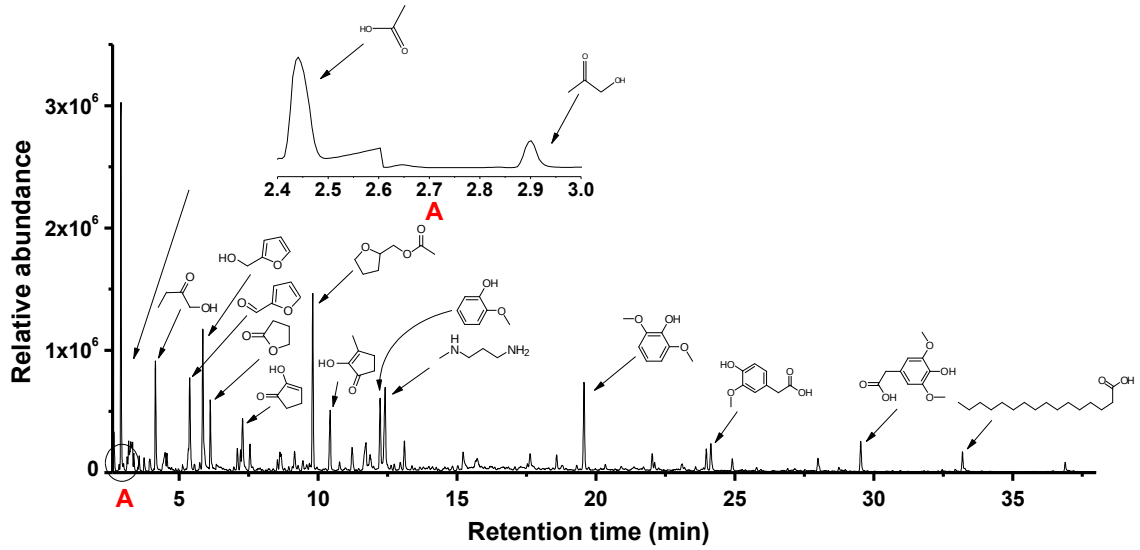

Fig. 4. Chromatogram of the GC-MS result for WSMC from CS co-pyrolysis

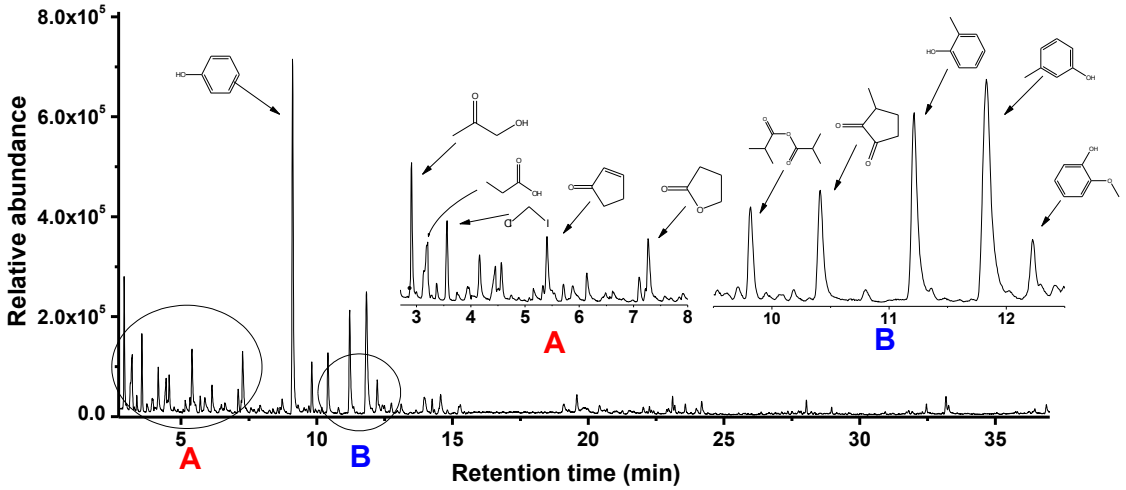

Fig. 5. GC-MS Chromatogram for WSMC from CS/SM co-pyrolysis at the ratio of 20/100

The co-pyrolysis interaction improved the formation of alcohols and ketones and reduced the yield of aldehydes, as shown in Fig. 2b. It is generally accepted that alcohols, ketones, and aldehydes are generated from the addition reaction of small molecule oxygen radicals (Collard and Blin 2014). There is competition between the formation of ketones and aldehydes. Because the radicals with C=O structure had more reactivity with alkyl radicals, the formation of ketones accelerated during co-pyrolysis. The formation of aldehydes was simultaneously inhibited. Moreover, alkyl radicals from SM pyrolysis encouraged the stabilization of small molecule oxygen radicals, most of which were from CS pyrolysis and produced more alcohols and ketones during co-pyrolysis. As can be seen in Fig. 4, the GC-MS result of CS pyrolysis had more furan peaks than did the co-pyrolysis. Hence, Fig. 2b shows that the yield of furans from co-pyrolysis was more than its calculated value. Most furans were generally derived from the cyclization reaction of a deoxidized cellulose unit during SM pyrolysis. The proper amount of alkyl radicals from SM pyrolysis could have restrained such cyclization reaction and reacted with the deoxidized cellulose unit to produce more C2-C4 hydrocarbons, as shown in Fig. 6. Because the radical reactions of WSMC formation consumed much more oxyradicals (such as hydroxyl radical), the water generation was restrained during co-pyrolysis (seen in Fig. 1).

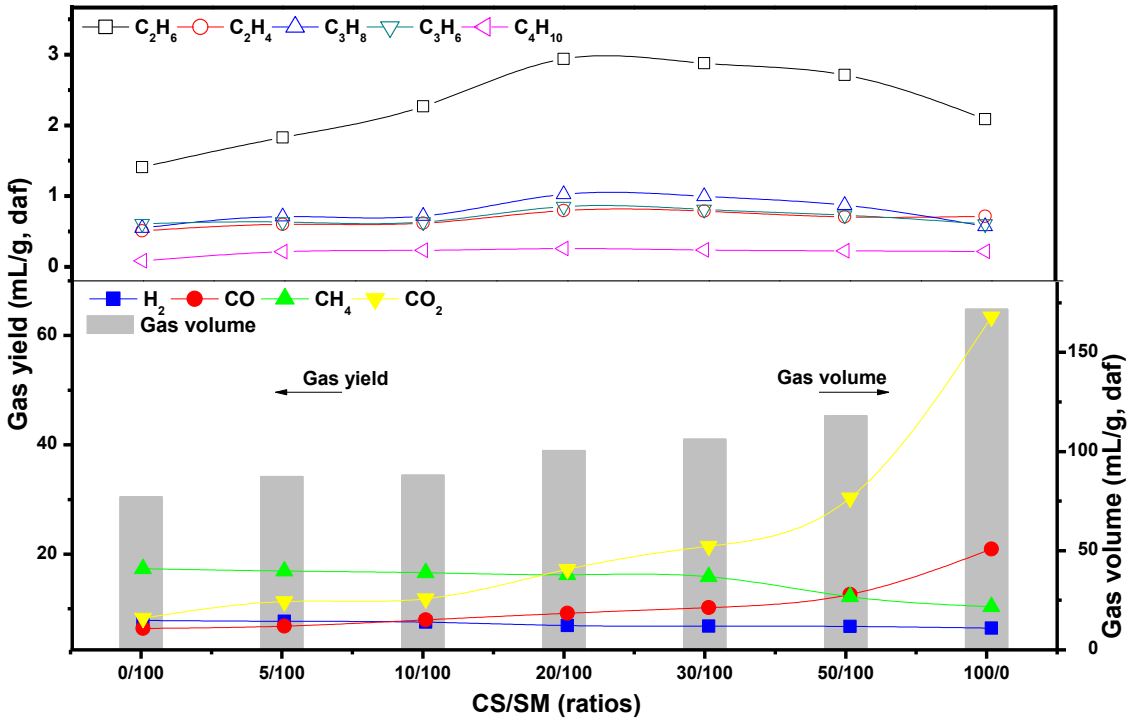

Fig. 6. GC analyses of syngas from pyrolysis

Syngas Characterization Derived from Pyrolysis

The GC results of syngas from pyrolysis are illustrated in Fig. 6. The syngas volume of SM pyrolysis was 77.13 mL/g (daf), and 22.51 (v/v%) of it was CH_4. CH_4 was mainly generated from the cleavage of the methyl side chain during SM pyrolysis. While CO_2 was the primary component in the syngas volume of CS pyrolysis (171.75 mL/g, daf) and its yield was 10.40 mL/g (daf), the second most component was CO (20.93 mL/g, daf). The CO_2 and CO in the syngas of CS pyrolysis were mainly derived from the decomposition of

the cellulose unit and the separated oxygen-containing functional groups. Furthermore, the H_2 yield of CS pyrolysis and SM pyrolysis were 7.90 mL/g (daf) and 6.48 mL/g (daf), respectively. As can be seen in Fig. 6, C2–C4 hydrocarbons were also detected in the syngas from SM pyrolysis and CS pyrolysis, but their content was relatively low. Through increasing the ratio of CS in the CS/SM blend, the CO_2 and CO yields increased, but the CH_4 and H_2 yields decreased during the co-pyrolysis of CS and SM. Nonetheless, the H_2 yield was less affected by the CS/SM blending ratio. The results further demonstrated that CH_4 mainly derived from SM, and most of both CO_2 and CO were generated from CS during co-pyrolysis. Specifically, the yields of C2–C4 hydrocarbons first increased and then decreased with the increase of the CS content in the blend. Moreover, the maximum yield of C2–C4 hydrocarbons occurred at a 20/100 ratio of CS/SM during co-pyrolysis. The decomposition of the cellulose unit was influenced by the alkyl radical, which was mostly derived from SM pyrolysis to produce more C2–C4 hydrocarbons. At the same time, the yield of furans decreased. This production showed that the co-pyrolysis interaction promoted the yields of C2–C4 hydrocarbons in syngas.

In summary, the interaction between CS and SM during co-pyrolysis significantly affected the products in terms of small molecule compounds. It is well known that furan comes mainly from cellulose decomposition during biomass pyrolysis (Gu *et al.* 2013). The oxygen-containing radicals from CS pyrolysis were easier to combine with the alkyl radical from SM pyrolysis during co-pyrolysis (Tang *et al.* 2016). This kind of reaction improved the yields of ketones and esters. The co-pyrolysis radicals of C2-C4 from SM generated more hydrocarbons than that of SM pyrolysis.

CONCLUSIONS

1. The interaction between the two fuel types notably affected the yield of small molecule compounds during the co-pyrolysis of cotton stalk (CS) and Shenmu coal (SM). The yields of water-soluble small molecule compounds (WSMC) and syngas were always higher than the relevant calculated values. Moreover, the generation of water was apparently inhibited and consistently lower than its calculated values during co-pyrolysis.
2. The gas chromatography – mass spectrometry (GC-MS) analyses showed that the constituents of WSMC were greatly influenced by the co-pyrolysis interaction. The yield of pyridines from co-pyrolysis (0.28 wt%, daf) was higher than that of CS pyrolysis (0.17 wt%, daf) and SM pyrolysis (0.06 wt%, daf). The phenols yield was 1.68 wt% (daf) and 25.60% higher than its calculated value in the WSMC from the co-pyrolysis of CS and SM. Compared with the calculated value, the co-pyrolysis also produced more alcohols. The yield of furans from co-pyrolysis was 0.10 wt% (daf) and only 25.64% as far as the calculated value based on separate pyrolysis results. Moreover, the esterification reaction was improved by co-pyrolysis interaction. As a result, the yield of esters increased, whereas the yield of carboxylic acids decreased accordingly. Acetic acid was not detected in the WSMC from CS/SM co-pyrolysis with a 20/100 CS/SM ratio. In addition, the co-pyrolysis interaction completely blocked the formation of amides and accelerated the generation of pyridine during co-pyrolysis.

3. CH_4 was the greatest component in the syngas of SM pyrolysis. Through increasing the CS of the ratio in blends, the yields of CO_2 and CO increased and the CH_4 yield decreased during the co-pyrolysis. The yields of C2–C4 hydrocarbons in co-pyrolysis syngas first increased and then decreased as well. The maximal yields of C2–C4 hydrocarbons all occurred with the 20/100 ratio of CS/SM because the generation of furans was restrained during co-pyrolysis.

ACKNOWLEDGEMENTS

This work was supported by the National Key Research and Development Projects of China (No. 2016YFB0600303), the Natural Science Foundation of Liaoning Province (No. 20180550636), and the Scientific Research Projects of Institutions of Higher Learning in Liaoning Province (No. 2019LNJC14).

REFERENCES CITED

Abdelsayed, V., Ellison, C. R., Trubetskaya, A., Smith, M. W., and Dushyant, S. (2019). "Effect of microwave and thermal co-pyrolysis of low-rank coal and pine wood on product distributions and char structure," *Energy & Fuels* 33(8), 7069-7082. DOI: 10.1021/acs.energyfuels.9b01105

Abnisa, F., and Daud, W. M. A. W. (2014). "A review on co-pyrolysis of biomass: An optional technique to obtain a high-grade pyrolysis oil," *Energy Conversion and Management* 87, 71-85. DOI: 10.1016/j.enconman.2014.07.007

ASTM D4006-16e1. (2016). "Standard test method for water in crude oil by distillation," ASTM International, West Conshohocken, PA, USA.

Collard, F. X., and Blin, J. (2014). "A review on pyrolysis of biomass constituents: Mechanisms and composition of the products obtained from the conversion of cellulose, hemicelluloses, and lignin," *Renewable and Sustainable Energy Reviews* 38, 594-608. DOI: 10.1016/j.rser.2014.06.013

Dong, C. Q., Zhang, Z. F., Lu, Q., and Yang, Y. P. (2012). "Characteristics and mechanism study of analytical fast pyrolysis of poplar wood," *Energy Conversion and Management* 57, 49-59. DOI: 10.1016/j.enconman.2011.12.012

Gu, X., Ma, X., Li, L., Liu, C., Cheng, K., and Li, Z. (2013). "Pyrolysis of poplar wood sawdust by TG-FTIR and Py–GC/MS," *Journal of Analytical and Applied Pyrolysis* 102, 16-23. DOI: 10.1016/j.jaap.2013.04.009

Hassan, H., Lim, J. K., and Hameed, B. H. (2016). "Recent progress on biomass co-pyrolysis conversion into high-quality bio-oil," *Bioresource Technology* 221, 645-655. DOI: 10.1016/j.biortech.2016.09.026

He, W. J., Liu, Q. Y., Shi, L., Liu, Z. Y., Ci, D. H., Lievens, C., Guo, X. F., and Liu, M. X. (2014). "Understanding the stability of pyrolysis tars from biomass in a view point of free radicals," *Bioresource Technology* 156, 372-375. DOI: 10.1016/j.biortech.2014.01.063

Krerkkaiwan, S., Fushimi, C., Tsutsumi, A., and Kuchonthara, P. (2013). "Synergetic effect during co-pyrolysis/gasification of biomass and sub-bituminous coal," *Fuel Processing Technology* 115, 11-18. DOI: 10.1016/j.fuproc.2013.03.044

Li, J. G., Zhu, J. L., Hu, H. Q., Jin, L. J., Wang, D. C., and Wang, G. J. (2020). "Co-pyrolysis of Baiyinhua lignite and pine in an infrared-heated fixed bed to improve tar yield," *Fuel* 272(3), Article ID 117739. DOI: 10.1016/j.fuel.2020.117739

Li, S., Chen, X., Wang, L., Liu, A., and Yu, G. (2013). "Co-pyrolysis behaviors of saw dust and Shenfu coal in drop tube furnace and fixed bed reactor," *Bioresource Technology* 148, 24-29. DOI: 10.1016/j.biortech.2013.08.126

Liang, X. M., Sun, X. B., Xu, J. T., and Ye, D. Q. (2020). "Improved emissions inventory and VOCs speciation for industrial OFP estimation in China," *Science of The Total Environment* 745, Article ID 140838. DOI: 10.1016/j.scitotenv.2020.140838

Lievens, C., Ci, D. H., Bai, Y., Ma, L. G., Zhang, R., Chen, J. Y., and Gai, Q. Q. (2013). "A study of slow pyrolysis of one low rank coal *via* pyrolysis–GC/MS," *Fuel Processing Technology* 116, 85-93. DOI: 10.1016/j.fuproc.2013.04.026

Liu, P., Zhang, D. X., Wang, L., Zhou, Y., Pan, T. Y., and Lu, X. L. (2016). "The structure and pyrolysis product distribution of lignite from different sedimentary environment," *Applied Energy* 163, 254-262. DOI: 10.1016/j.apenergy.2015.10.166

Lu, K. M., Lee, W. J., Chen, W. H., and Lin, T. C. (2013). "Thermogravimetric analysis and kinetics of co-pyrolysis of raw/torrefied wood and coal blends," *Applied Energy* 105, 57-65. DOI: 10.1016/j.apenergy.2012.12.050

Malen, J., and Marcus, A. A. (2017). "Promoting clean energy technology entrepreneurship: The role of external context," *Energy Policy* 102, 7-15. DOI: 10.1016/j.enpol.2016.11.045

Meng, J. J., Moore, A., Tilotta, D. C., Kelley, S. S., Adhikari, S., and Park, S. (2015). "Thermal and storage stability of bio-oil from pyrolysis of torrefied wood," *Energy & Fuels* 29(7), 5117-5126. DOI: 10.1021/acs.energyfuels.5b00929

Sonobe, T., Worasuwannarak, N., and Pipatmanomai, S. (2008). "Synergies in co-pyrolysis of Thai lignite and corncob," *Fuel Processing Technology* 89(12), 1371-1378. DOI: 10.1016/j.fuproc.2008.06.006

Tang, C. Y., and Zhang, D. X. (2016). "Mechanisms of aliphatic hydrocarbon formation during co-pyrolysis of coal and cotton stalk," *Chinese Chemical Letters* 27(10), 1607-1611. DOI: 10.1016/j.cclet.2016.03.037

Tang, C. Y., Zhang, D. X., and Lu, X. L. (2015). "Improving the yield and quality of tar during co-pyrolysis of coal and cotton stalk," *BioResources* 10(4), 7667-7680. DOI: 10.15376/biores.10.4.7667-7680

Wei, J., Gong, Y., Guo, Q., Ding, L., Wang, F., and Yu, G. (2017). "Physicochemical evolution during rice straw and coal co-pyrolysis and its effect on co-gasification reactivity," *Bioresource Technology* 227, 345-352. DOI: 10.1016/j.biortech.2016.12.068

Weiland, N. T., Means, N. C., and Morreale, B. D. (2012). "Product distributions from isothermal co-pyrolysis of coal and biomass," *Fuel* 94, 563-570. DOI: 10.1016/j.fuel.2011.10.046

Wu, Z. Q., Wang, S. Z., Zhao, J., Chen, L., and Meng, H. Y. (2015). "Product distribution during co-pyrolysis of bituminous coal and lignocellulosic biomass major components in a drop-tube furnace," *Energy & Fuels* 29(7), 4168-4180. DOI: 10.1021/acs.energyfuels.5b00374

Yang, X., Yuan, C., Xu, J., and Zhang, W. (2014). "Co-pyrolysis of Chinese lignite and biomass in a vacuum reactor," *Bioresource Technology* 173, 1-5. DOI: 10.1016/j.biortech.2014.09.073

Zhang, L., Xu, S., Zhao, W., and Liu, S. (2007). "Co-pyrolysis of biomass and coal in a free fall reactor," *Fuel* 86(3), 353-359. DOI: 10.1016/j.fuel.2006.07.004

Zhu, J. L., Jin, L. J., Luo, Y. W., Hu, H. Q., Xiong, Y. K., Wei, B. Y., and Wang, D. C. (2020). "Fast co-pyrolysis of a massive Naomaohu coal and cedar mixture using rapid infrared heating," *Energy Conversion and Management* 205, Article ID 112442. DOI: 10.1016/j.enconman.2019.112442

Article submitted: November 7, 2020; Peer review completed: January 2, 2021; Revised version received and accepted: January 7, 2021; Published: January 8, 2021.
DOI: 10.15376/biores.16.1.1469-1481